

**Title: Tandem proxy evidence demonstrates glacial expansion of oxygen
depleted seawater in the eastern tropical Pacific**

Authors: Babette, A.A. Hoogakker^{1,2*}, Zunli Lu^{3,4*}, Natalie Umling⁵, Luke Jones², Xiaoli Zhou⁶, Ros E.M. Rickaby², Robert Thunell⁵, Olivier Cartapanis⁷, Eric Galbraith^{8,9}.

Affiliations:

* Corresponding author

¹ The Lyell Centre, Heriot-Watt University, Research Avenue South, EH14 4AP, Edinburgh, UK.

² Department of Earth Sciences, University of Oxford, South Parks Road, OX1 3AN, Oxford, UK.

³ Department of Earth Sciences, 310 Heroy Geology Laboratory, Syracuse University, Syracuse, NY 13244-1070 USA.

⁴ State Key Laboratory of Marine Environmental Science, Xiamen University, Xiamen 361102, China.

⁵ School of Earth, Ocean and Environment, University of South Carolina, 701 Sumter Street, EWS 617, Columbia, SC 29208 USA.

⁶ Department of Marine and Coastal Sciences, Rutgers University, 71 Dudley Rd, New Brunswick, NJ 08901, USA

⁷ University of Bern, Oeschger Centre for Climate Change Research, Falkenplatz 16, CH-3012 Bern, Switzerland.

⁸ Institut de Ciència i Tecnologia Ambientals (ICTA) and Department of Mathematics, Universitat Autònoma de Barcelona, Carrer de les Columnes, 08193 Bellaterra, Spain.

⁹ ICREA, Pg. Lluís Companys 23, 08010 Barcelona, Spain

Summary:

The oceanic concentrations of dissolved oxygen and carbon dioxide are intimately coupled through the production and respiration of organic matter, and can vary with climate due to changes in ecosystem functioning and ocean circulation (Schmidtko). Marine sediment proxy records have suggested that oxygen concentrations in the deep ocean were lower during the last ice age. This observation is consistent with greater oceanic carbon storage contributing to lower atmospheric CO₂ (Sigman2000,Jaccard2009Hoogakker2014). At the same time, it has

been suggested that the poorly-oxygenated near-surface and intermediate waters of the Pacific Ocean, the largest ocean basin, were generally better-oxygenated during the glacial⁵⁻⁷, which could imply a minimal net basin-integrated change in carbon storage. Here we apply a novel dual-proxy approach, incorporating qualitative upper water-column oxygen and quantitative bottom water oxygen reconstructions^{3, 4}, to constrain changes in the vertical extent of low oxygen waters in the eastern tropical Pacific in response to large-scale climate change since the last ice age. Our tandem proxy reconstructions provide evidence of a downward expansion of oxygen depletion in the eastern Pacific during the last glacial due to increased oxygen utilization, with no sign of greater oxygenation in the upper reaches of the water column. We extrapolate our quantitative deep oxygen reconstructions using widely-distributed epibenthic carbon isotope measurements, to show that the glacial increase of the Pacific respired carbon reservoir was a major player in the glacial-interglacial CO₂ cycles.

One Sentence Summary:

During the last ice age, oxygen depletion expanded from subsurface to deep waters in the eastern tropical Pacific, indicating a net increase in its respired carbon reservoir.

Main Text:

The Pacific Ocean contains a vast volume of oxygen-depleted waters. In the eastern basin, north of 18°S, waters deeper than 1 km (deepening to 2 km north of the equator) are generally oxic ([O₂] >120 μmol/kg), whereas above this most waters are hypoxic ([O₂] <120 μmol/kg), and a small fraction are suboxic ([O₂] < 2 to 10 μmol/kg)⁸. The eastern tropical North Pacific (ETNP) oxygen minimum zone (OMZ) is the world's largest OMZ, encompassing 67% of total suboxic waters⁸. Low oxygen conditions place important limitations on marine life with hypoxic conditions proving lethal for more than 50% of marine benthic animals⁹. Oceanic

nutrient cycling is also affected by suboxic conditions^{10, 11}, under which remineralization of organic material occurs via anaerobic metabolic pathways, including denitrification and anammox. This removes bioavailable nitrogen (which supports primary production) from the ocean and generates the greenhouse gas N₂O.

Because of the intrinsic link between oxygen and carbon during photosynthesis and respiration, oxygen utilization provides a direct reflection of the strength of the biological carbon pump and therefore its influence on atmospheric CO₂ (ref. 4). Today the Pacific Ocean represents the largest modern sink of respired organic carbon (>730 Gt, ~50% of the global ocean inventory¹²), half of which resides in the upper 1.5 km.

The concentration of dissolved oxygen in seawater is controlled by (i) the saturation oxygen concentration in contact with the atmosphere, which is a function of temperature and salinity, and (ii) net oxygen utilization, which is determined by any initial disequilibrium from saturation at the ocean surface plus the accumulated consumption during remineralization of organic material along the pathways of advection and mixing¹⁰. Over the last 50 years an observed vertical expansion of the equatorial Pacific OMZ has been attributed to net increased oxygen utilization, which could reflect a reduced input rate of oxygen through advection and mixing and/or an increase in the local rate of organic matter respiration^{1, 13}. A further decline in ocean oxygen levels is predicted by Earth system models under anthropogenic warming, linked to increased temperatures (lowering saturation oxygen concentration) and increased oxygen utilization due decreased ventilation^{1, 10, 14}. However, model simulations disagree about oxygen changes in the tropical thermoclines, and do not reproduce the large historical changes¹, suggesting these models are missing important processes that may compromise their predictions of future change¹⁴.

Reconstructions of the last ice age offer an alternative test of the link between climate and ocean oxygenation. Lower glacial seawater temperatures would have increased oxygen

saturation concentrations⁷ and decreased remineralization rates¹⁵. These conditions could have resulted in a better oxygenated upper ocean, potentially eliminating the OMZs. Bulk sedimentary nitrogen isotope ($\delta^{15}\text{N}$) records from the eastern tropical Pacific (ETP)^{16, 17} have been interpreted to reflect overall reduced glacial denitrification rates in the upper water column¹⁸, which could indicate an absence of suboxic waters. In contrast, the cold-enhanced solubility appears to have been overwhelmed by increased oxygen utilization in the deep Pacific, resulting in reduced oxygen concentrations and increased respired carbon storage that could have contributed to the low atmospheric CO_2 concentrations⁵⁻⁷. However, these reconstructions are based on qualitative proxies, which are often difficult to interpret¹⁹. Furthermore, many of these records have been limited to core sites from continental slopes, and are potentially biased by local conditions¹⁹. Here we apply a novel dual-proxy approach to constrain changes in the upper and lower boundaries of the presently-oxygen-depleted water column of the eastern tropical Pacific since the last glacial period.

To constrain upper-water column oxygen concentrations, we utilized planktonic foraminifera I/Ca^3 . This proxy takes advantage of iodine speciation in seawater. The iodate species (IO_3^-) is favoured under well-oxygenated settings, whereas iodide (I^-) becomes the dominant species under oxygen-depleted conditions. Foraminiferal calcite only incorporates iodate, so that foraminiferal I/Ca reflects the abundance of the oxidised form²⁰.

Furthermore, we utilize the benthic foraminiferal carbon isotope gradient proxy ($\Delta\delta^{13}\text{C}$) to quantitatively reconstruct bottom water oxygen concentrations⁴. The $\Delta\delta^{13}\text{C}$ between bottom water and pore-water at the anoxic boundary in sediments is related to the oxygen concentration of the overlying bottom waters²¹. The $\Delta\delta^{13}\text{C}$ between bottom water and pore-water at the anoxic boundary is reproduced by the $\Delta\delta^{13}\text{C}$ of benthic foraminifera with microhabitats in bottom water (*Cibicidoides wuellerstorfi*) and in sediments at the anoxic boundary (*Globobulimina spp.*)⁴. This method allows us to quantitatively reconstruct

dissolved oxygen concentrations in the range of 55 to 235 $\mu\text{mol/kg}$ (see methods) in bottom waters from tropical to temperate regions, with an estimated total standard error of 17 $\mu\text{mol/kg}^4$. Our tandem proxy approach allows us to place firm constraints on past changes in the geometry of oxygen depleted waters in the eastern tropical Pacific over the last 40,000 years. Furthermore, extrapolation of our new quantitative bottom water oxygen reconstructions allows us to calculate the change in the size of the Pacific respired carbon pool and assess its role in glacial-interglacial CO_2 cycles.

Planktonic foraminifera I/Ca ratios were measured at two eastern tropical Pacific sites. Site ODP 1242 (7.86°N, 83.61°W, 1.36 km) is on the Costa Rica margin, in the eastern tropical North Pacific (ETNP), while ODP 849 (0.18°N, 110.50°W, 3.85 km) lies beneath the eastern equatorial cold tongue (Fig. 1). Planktonic foraminifera I/Ca ratios at the ETNP site are expected to monitor changes in the upper boundary of ETNP-OMZ. The cold tongue Site ODP 849 is distal from modern suboxic zones but downstream of waters that have passed through them, and planktonic foraminifera I/Ca ratios at this location are expected to have responded to the broader presence of oxygen depleted waters within the ETP-OMZ. The location of ODP 1242 at the deep boundary of the present day ETNP-OMZ is ideal to test for changes in the vertical extent of the OMZ, via benthic foraminifera $\Delta\delta^{13}\text{C}$. Additionally, bottom water oxygen concentrations were reconstructed for deep water at TR163-25 (1.65°S, 88.45°W, 2.65 km), to provide quantitative estimates of changes in deep water oxygen concentrations in the eastern tropical Pacific and calculate the glacial increase in the deep Pacific respired carbon pool. Details of age models are provided in the methods section and Fig 4.

Modern oxygen profiles at ODP Sites 849 and 1242 are very similar (Fig. 1), except that OMZ waters ($[\text{O}_2]$ threshold $< 45 \mu\text{mol/kg}^{22}$) occur at a much shallower depth (within the upper 50m) at the ETNP site compared to the cold tongue site (deeper than 250 m) (Fig. 1).

This upper water column difference is consistent with the contrasting core-top planktonic foraminifera I/Ca values at the two sites (Fig. 2). If suboxia had been reduced during the glacial, as has been previously argued, one would expect higher I/Ca to be found in glacial-age foraminifera. Instead we find that low I/Ca ($<0.6 \mu\text{mol/mol}$) prevailed continuously over the last 40 kyr at the ETNP-OMZ site, consistent with persistent oxygen depletion at shallow depths (Fig. 2). Furthermore, although I/Ca ratios of all planktonic species in the cold tongue from 40-25 ka BP were similar to late Holocene values, during early deglaciation (~18-16 ka BP) the I/Ca of shallow dwelling species fell to values as low as the thermocline species. Persistently depleted planktonic foraminifera oxygen isotopes values of the shallow dwelling species and heavy values of the thermocline species (Fig. 2) indicate similar depth habitats over the last 40,000 years. Therefore, the lower I/Ca values of the shallow dwelling species at Site 849 during early deglaciation are interpreted to be due to an increased presence of oxygen-depleted waters in the ETP-OMZ.

Turning to the deep sea, reconstructed dissolved oxygen at ODP Site 1242 shows generally lower concentrations during the glacial compared to the Holocene, with an average LGM (18 to 22 ka BP) dissolved oxygen content of $55 \mu\text{mol/kg}$ ($\pm 17 \mu\text{mol/kg}$, Fig. 3). The lowest oxygen concentrations ($44 \mu\text{mol/kg}$) were recorded during early deglaciation, (17 to 15 ka BP), followed by a rapid increase in the mid-late deglaciation. Maximum oxygen concentrations of $100 \mu\text{mol/kg}$ were recorded during the early Holocene. Oxygenation then decreased slightly through the Holocene, reaching late Holocene values of $85 \mu\text{mol/kg}$ (Fig. 3). At the deeper site TR163-25, reconstructed LGM oxygen concentrations are similar to ODP Site 1242, averaging $54 \mu\text{mol/kg}$ (Fig. 3), and there is also a brief decline in dissolved oxygen during the early deglaciation to $\sim 40 \mu\text{mol/kg}$ followed by a rapid increase to $\sim 160 \mu\text{mol/kg}$ in the mid-Holocene (Fig. 3).

Our dual-proxy results from the upper 1.4 km of the water column (planktonic foraminifera I/Ca at ODP Sites 1242 & 849, $\Delta\delta^{13}\text{C}$ at ODP Site 1242) show sustained oxygen depletion that contrasts with other studies that have suggested the upper water column in the Pacific was generally more oxygenated at this time⁵⁻⁷. These prior conclusions were based on observations of low sedimentary $\delta^{15}\text{N}$ (interpreted as lower rates of denitrification), weaker sedimentary laminations and lower oxygen-sensitive trace metal abundances during the glacial⁷. However, as we explain in our method section (e.g. see Fig. 5) there are several reasons that sedimentary $\delta^{15}\text{N}$ could have been lower during the glacial without a significant change in oxygen concentrations. Furthermore, the sedimentary laminations and trace metals previously examined at three sites in the coastal ETP showed only weak signs of oxygen change between the LGM and Holocene^{16,17}, which could also be attributed to changes in the characteristics of accumulating sediments^{26,27}. Thus, the persistently low I/Ca values, in combination with lowered glacial bottom water oxygen levels at 1.4 km (today the lower boundary of the ETNP-OMZ), do not support a significant contraction of the upper reaches of the tropical Pacific OMZ during the glacial period compared to today.

Our results also indicate a period of particularly strong oxygen depletion during the early deglaciation, consistent with prior sedimentary $\delta^{15}\text{N}$, lamination, and trace metal evidence from the ETNP^{16,17}. The convergence of mixed layer and thermocline planktonic foraminifera to low values of I/Ca at ODP Site 849 (Fig. 2) suggests that the downward expansion of oxygen depleted waters in the ETP-OMZ indicated by the bottom water oxygen reconstructions (Fig. 3), was accompanied by an intensified influence of oxygen depleted-waters in the upper water column. The interval coincides with a weak Atlantic Meridional Overturning Circulation, and an apparent productivity peak in the eastern equatorial Pacific speculated to reflect increased delivery of nutrients from southern-sourced deep waters and intensified upwelling^{17, 28, 29,30}.

Our tandem proxy results provide new insights into the evolution of respired carbon storage in the eastern tropical Pacific since the last ice age. Today half of the total global respired carbon reservoir is stored in intermediate and subsurface waters of the Pacific (e.g. upper 1.5 km). Our results suggest little LGM-Holocene change in the respired carbon reservoir of the upper water column, but an increase of the deeper Pacific respired reservoir, implying a net increase in the size of the Pacific glacial respired pool. Furthermore, our $\Delta\delta^{13}\text{C}$ results show that the modern vertical oxygen gradient ($\Delta[\text{O}_2]$ of $\sim 65 \mu\text{mol/kg}$) between water depths of 1.4 and 2.6 km was eliminated during the LGM (Fig 1), so that oxygen concentrations did not increase with depth as they do today. We also find that the gradient in $\delta^{13}\text{C}$ of DIC between these water masses was reversed (methods Fig. 6), as would be expected given the respired carbon concentrations inferred from our quantitative oxygen reconstructions, and similar changes in the preformed component of $\delta^{13}\text{C}$ (for details see Methods). Our data therefore show that, despite large changes in average $\delta^{13}\text{C}$ of DIC for the whole ocean and changes air-sea exchange, the relative change in $\delta^{13}\text{C}$ between sites in the 1.4 - 3 km depth range provides a good approximation of oxygen change.

We take advantage of this new constraint together with our LGM-modern $\delta^{13}\text{C}$ compilation to extrapolate our results spatially in the deep Pacific. Our results suggest that the total amount of respired carbon (i.e. that associated with oxygen utilization) in the Pacific increased by 90 Gt C between water depths of 1.4 and 3 km, and possibly 196 Gt C across the whole of the deep Pacific (methods). This provides a powerful new target for model simulations of glacial carbon cycling. Whilst the average increase in respired carbon concentrations in deeper waters of the Pacific is only half that of the deep Atlantic³, the estimated glacial increase in its respired carbon reservoir is almost three times that of the

deep Atlantic due to its vast size. This suggests that the Pacific made an important contribution to the glacial-interglacial changes of atmospheric CO₂ levels.

References:

1. Schmidtko, S., Stramma, L., Visbeck, M. Decline in global oceanic oxygen content during the past five decades. *Nature* **542**, 335-229 (2017).
2. Long, M., Deutsch, C., Ito, I. Finding forced trends in oceanic oxygen. *Glob. Biogeochem. Cycles* **30**, 318-397 (2016).
3. Lu, Z., Hoogakker, B.A.A., Hillenbrand, C.-D., Zhou, X., E. Thomas, E., et al. Oxygen depletion recorded in upper waters of the glacial Southern Ocean. *Nat. Comm.* **7**, 11146 (2016).
4. Hoogakker, B.A.A., Elderfield, H., Schmiedl, G., McCave, I.N., Rickaby, R.E.M. Glacial-interglacial changes in bottom-water oxygen content on the Portuguese margin. *Nat. Geosci.* **8**, 40-43 (2015).
5. Sigman, D.M., Boyle, E.A. Glacial/interglacial variations in atmospheric carbon dioxide. *Nature* **407**, 859-869 (2000).
6. Bradtmiller, L.I., Anderson, R.F., Sachs, J.P., Fleisher, M.Q. A deeper respired carbon pool in the glacial equatorial Pacific Ocean. *Earth Planet. Sc. Lett.* **299**, 417-425 (2010).
7. Galbraith, E.D., Jaccard, S.L. Deglacial weakening of the oceanic soft tissue pump: global constraints from sedimentary nitrogen isotopes and oxygenation proxies. *Quaternary Sci. Rev.* **109**, 38-48 (2015).

8. Bianchi, D., Dunne, J.P., Sarmiento, J.L., Galbraith, E.D. Data-based estimates of suboxia, denitrification, and N₂O production in the ocean and their sensitivities to dissolved O₂. *Glob. Biogeochem. Cycles* **26**, doi:10.1029/2011GB004209 (2012).
9. Vaquer-Sunyer, R., Duarte, D.M. Thresholds of hypoxia for marine biodiversity. *PNAS* **105**, 14352-15457 (2008).
10. Keeling, R., Körtzinger, A., Gruber, N. Ocean deoxygenation in a warming world. *Annu. Rev. Mar. Sci.* **2**, 199-229 (2010).
11. Lam, P., Kuypers, M.M.M. Microbial nitrogen cycling processes in oxygen minimum zones. *Annu. Rev. Mar. Sci.* **3**, 317-345 (2011).
12. Schmittner, A., Somes, C.J. Complementary constraints from carbon (¹³C) and nitrogen (¹⁵N) isotopes on the glacial ocean's soft-tissue biological pump. *Paleoceanography* **31**, 669-693 (2016).
13. Stramma, L., Johnson, G.C., Sprintall, J., Mohrholz, V. Expanding oxygen-minimum zones in the tropical oceans. *Science* **320**, 656-658 (2008).
14. Bopp, L., Resplandy, L., Orr, J.C., Doney, S.C., Dunne, J.P., Gehlen, M., Halloran, P., Heinze, C., Ilyina, T., Séférian, R., Tjiputra, J., Vichi, M. Multiple stressors of ocean ecosystems in the 21st century: projections with CMIP5 models. *Biogeosciences* **10**, 6225-6245 (2013).
15. Matsumoto, K. Biology-mediated temperature control on atmospheric pCO₂ and ocean biogeochemistry. *Geophys. Res. Lett.* **34**, doi:10.1029/2007GL031301 (2007).
16. Pichevin, L.E., Ganashram, R.S., Francavilla, S., Arellano-Torres, E., Pedersen, T.F., Beaufort, L. Interhemispheric leakage of isotopically heavy nitrate in the eastern tropical Pacific during the last glacial period. *Paleoceanography* **25**, PA1204 (2010).

17. Hendy, I.L., Pedersen, T.F. Oxygen minimum zone expansion in the eastern tropical North Pacific during deglaciation. *Geophys. Res. Lett.* **33**, L20602 (2006).
18. Galbraith, E.D., Kienast, M., and the NICOPP working group members. The acceleration of ocean denitrification during deglacial warming. *Nat. Geosci.* **6**, 579-584 (2013).
19. Moffit, S.E., Moffit, R.A., Sauthoff, W., Davis, C.V., Hewett, K., Hill, T.M. Paleoceanographic insights on recent oxygen minimum zone expansion: lessons for modern oceanography. *PLoS ONE* **10**, doi:10.1371/journal.pone.0115246 (2015).
20. Lu, Z., Jenkyns, H.C., Rickaby, R.E.M. Iodine to calcium ratios in marine carbonates as a paleo-redox proxy during oceanic anoxic events. *Geology* **38**, 1107-1110 (2010).
21. McCorkle, D.C., Emerson, S.R. The relationship between pore water carbon isotopic composition and bottom water oxygen concentration. *Geochim. Cosmochim. Acta* **52**, 1169-1178 (1988).
22. Karstensen, J., Stramma, L., Visbeck, M. Oxygen minimum zones in the eastern tropical Atlantic and Pacific oceans. *Prog. Oceanogr.* **77**, 331-350 (2008).
23. Stern, J.V., Lisiecki, L.E. Termination 1 timing in radiocarbon-dated regional benthic $\delta^{18}\text{O}$ stacks. *Paleoceanography* **29**, 1127-1142 (2014).
24. Benway, H.M., Mix, A.C., Haley, B.A., Klinkhammer, G.P. Eastern Pacific warm pool paleosalinity and climate variability: 0-30 kyr. *Paleoceanography* **21**, PA3008 (2006).
25. Eide, M., Olsen, A., Ninnemann, U.S., Eldevik, T. A global estimate of the full oceanic ^{13}C Suess effect since the preindustrial *Glob. Biogeochem. Cycles* **31**, 492–514 (2017).
26. van Geen, A., Zheng, Y., Bernhard, M., Cannariato, K.G., Carriguiry, J., Dean, W.E., Eakins, B.W., Ortiz, J.D., Pike, J. On the preservation of laminated sediments along the

western margin of North America. *Paleoceanography* **18**, doi:10.1029/2003PA000911
(2003).

27. Nameroff, T.J., Calvert, E., Murray, J.W. Glacial-interglacial variability in the eastern
tropical North Pacific oxygen minimum zone recorded by redox-sensitive trace metals.
Paleoceanography **19**, doi:10.1029/2003PA000912 (2004).

28. Costa, K.M., Jacobel, A.W., McManus, J.F., Anderson, R.F., Winckler, G., Thiagarajan,
N. Productivity patterns in the Equatorial Pacific over the last 30,000 years. *Glob.
Biogeochem. Cycles* **31**, 850-865 (2017).

29. Kienast, M., Kienast, S.S., Calvert, S.E., Eglinton, T.I., Mollenhauer, G., Francois, R.,
Mix, A.C. Eastern Pacific cooling and Atlantic overturning circulation during the last
deglaciation. *Nature* **443**, 846-849.

30. de la Fuente, M., Skinner, L., Calvo, E., Pelejero, C., Cacho, I. Increased reservoir ages
and poorly ventilated deep waters inferred in the glacial Eastern Equatorial Pacific. *Nat.
Comm.* **6**, 7420 (2015).

Acknowledgments: This work benefitted greatly from discussions with Raja Ganeshram.

This work is supported by UK Natural Environment Research Council (NERC) grant
NE/I020563/1 (to BAAH) and National Science Foundation (NSF) OCE-1232620,
OCE-1736542 (to ZL). This research used samples and/or data provided by the Ocean
Drilling Program (ODP). ODP is sponsored by the U.S. National Science Foundation
and participating countries (Natural Environment Research Council in UK) under
management of Joint Oceanographic Institutions (JOI), Inc. Mike Hall, James Rolfe

(University of Cambridge) and Chris Day (University of Oxford) are thanked for help
with stable isotope analyses.

Author contributions: BAAH and ZL conceived and coordinated the work. BAAH, ZL,
NU, LJ, XZ carried out data analyses; OC carried out data synthesis. BAAH and ZL
constructed the figures and wrote the paper, with contributions from the other co-
authors.

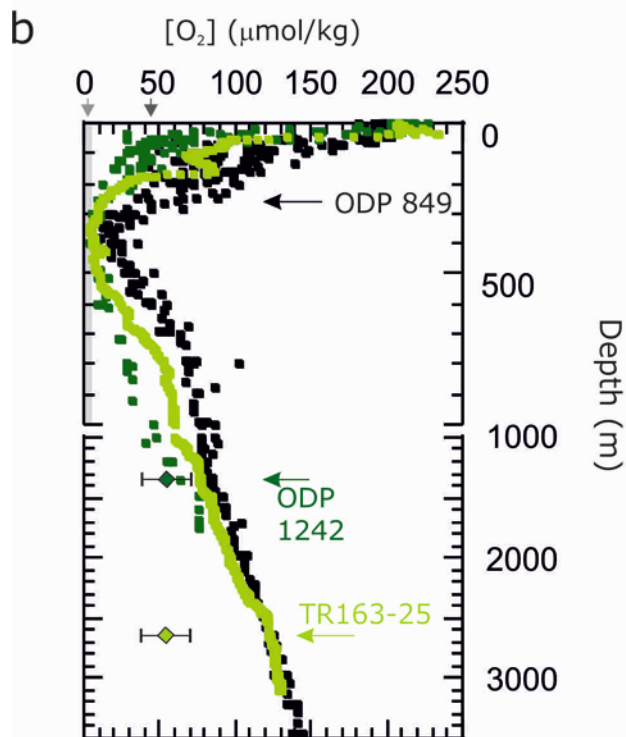
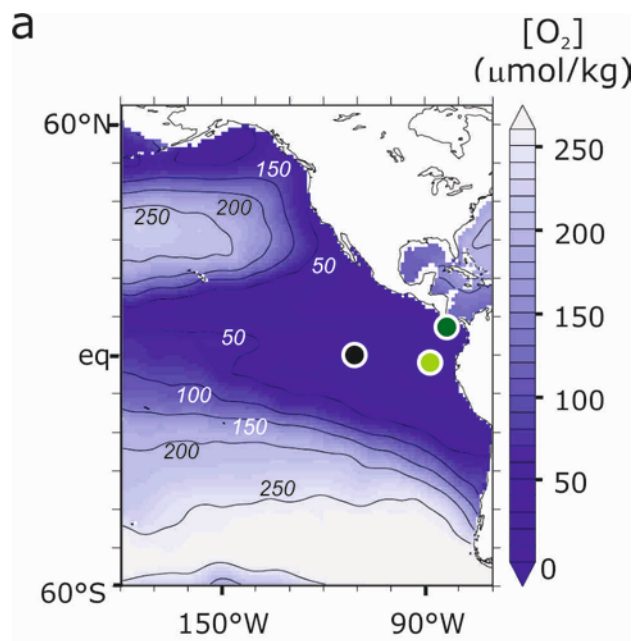
Figure captions

Figure 1. Overview of dissolved oxygen concentrations ([O₂]) in the eastern Pacific Ocean.

a, seawater [O₂] between 60°S and 60°N at 400 m water depth in the eastern equatorial Pacific, and locations of the three cores featuring in our study: ODP Site 1242 (dark green), 849 (black) and TR163-25 (light green). **b**, vertical seawater [O₂] profiles at the core sites (from <https://www.nodc.noaa.gov/OC5/SELECT/dbsearch/dbsearch.html>): ODP Site 1242 (dark green), ODP Site 849 (black) and TR163-25 (light green). Note different scale for upper part (0-1000 m) and lower part (1000-4000 m) of the water column. Base of thermocline is ~ 75 to 100 m. Arrows on the upper x-axis indicate [O₂] thresholds for suboxia (light grey) and the OMZ (dark grey). Diamonds illustrate reconstructed LGM bottom water [O₂] values at ODP Site 1242 and TR163-25, including $\pm 17 \mu\text{mol/kg}$ error⁴.

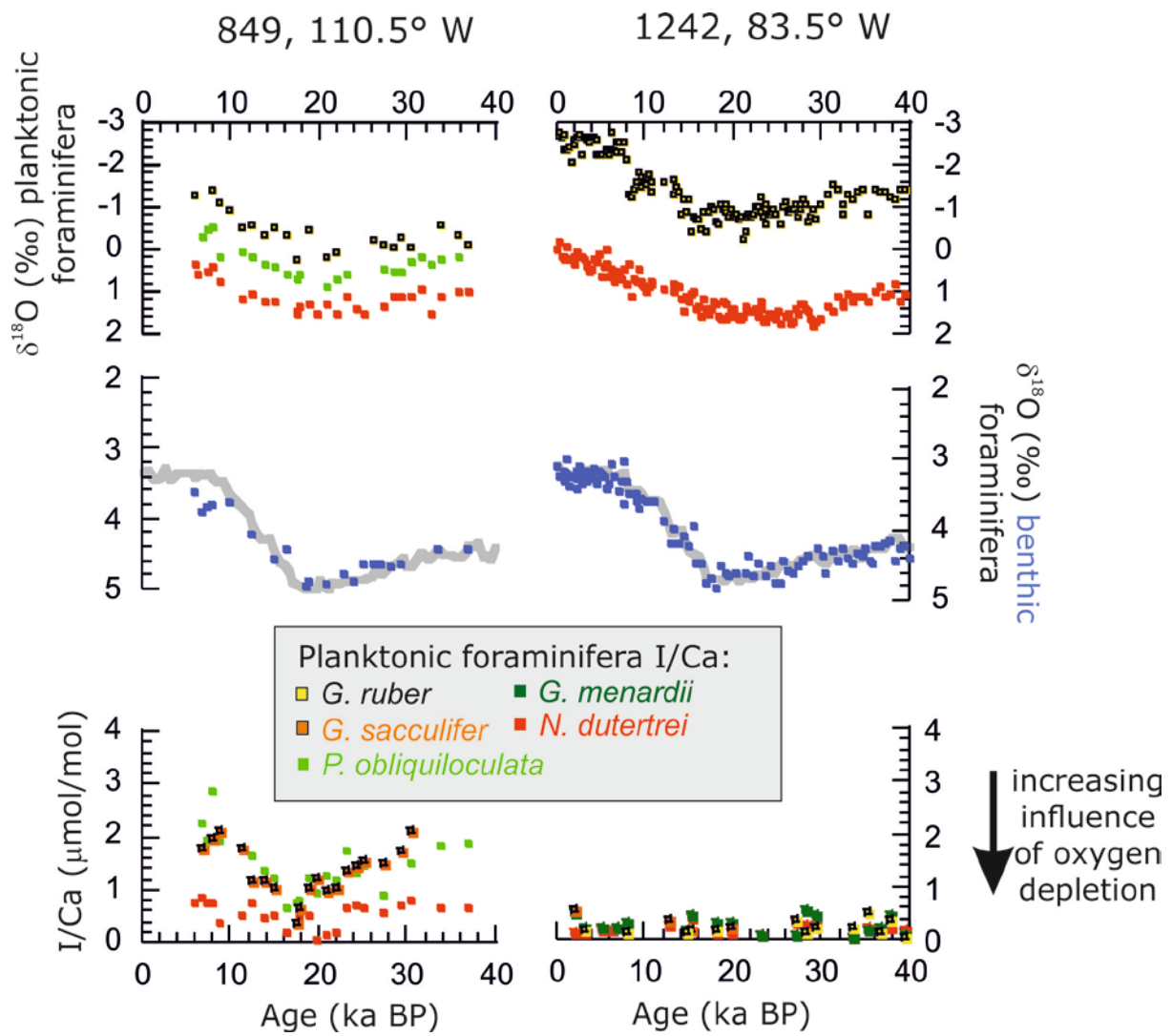
Figure 2. Reconstructed ETP surface water oxygenation. **a**, planktonic foraminiferal oxygen isotopes (red *Neogloboquadrina dutertrei*, light green *Pulleniatina obliquiloculata*, yellow *Globigerinoides ruber*) at ODP Sites 849 and 1242, with their composite benthic oxygen isotope records (blue symbols) and stacked records (grey lines)²³. The benthic composite $\delta^{18}\text{O}$ record of ODP Site 849 features specimens of *C. wuellerstorfi*, *Laticarinina pauperata* (both adjusted by +0.64‰ to bring it closer to values of *Uvigerina* spp.), and *Uvigerina* spp. The composite record of ODP Site 1242 $\delta^{18}\text{O}$ includes mainly specimens of *C. wuellerstorfi*, *Cibicidoides pachyderma*, and minor *Uvigerina peregrina*. Planktonic foraminiferal oxygen isotopes at 1242 until 28 ka BP are from²⁴. **b**, I/Ca ratios of planktonic foraminifera (red *N. dutertrei*, light green *P. obliquiloculata*, dark green *Globorotalia menardii*, yellow *G. ruber*, orange *Globigerinoides sacculifer*) at ODP Site 849 (left) and 1242 (right). I/Ca ratios < 2.5 $\mu\text{mol/mol}$ are indicative of the presence of low oxygen waters in the upper 400 m of the water column³.

Figure. 3. Reconstructed ETP bottom water oxygen concentrations. **a**, benthic foraminiferal oxygen isotopes (blue symbols) of ODP Site 1242 (composite record, see description Fig. 2) and TR163-25 (*C. wuellerstorfi*) with stacked benthic oxygen isotope records (grey lines) of the intermediate and deep Pacific from²³. Details of age models can be find in the methods section. **b**, benthic foraminiferal carbon isotopes of *C. wuellerstorfi* (red) and spp. *Globobulimina* (blue). **c**, reconstructed bottom water [O₂]/ $\Delta\delta^{13}\text{C}$ (raw data black squares + total error of $\pm 17 \mu\text{mol/kg}^4$, thick line shows moving average calculated using the boxcar algorithm). Yellow boxes: modern range of bottom water oxygen concentrations. At ODP Site 1242 one data point from ~38 ka BP fell outside of the calibration (reconstructed [O₂] 16 $\mu\text{mol/kg}$) and is not shown. The most recent Holocene is missing from core 1242, as evidenced by high core top $\delta^{13}\text{C}$ of *C. wuellerstorfi*, (average 0.4‰ top 25 cm) in contrast with seawater $\delta^{13}\text{C}$ of dissolved inorganic carbon (DIC) of -0.2 to -0.3‰²⁵. At TR163-25 the late Holocene (< 3,500 years) is missing.



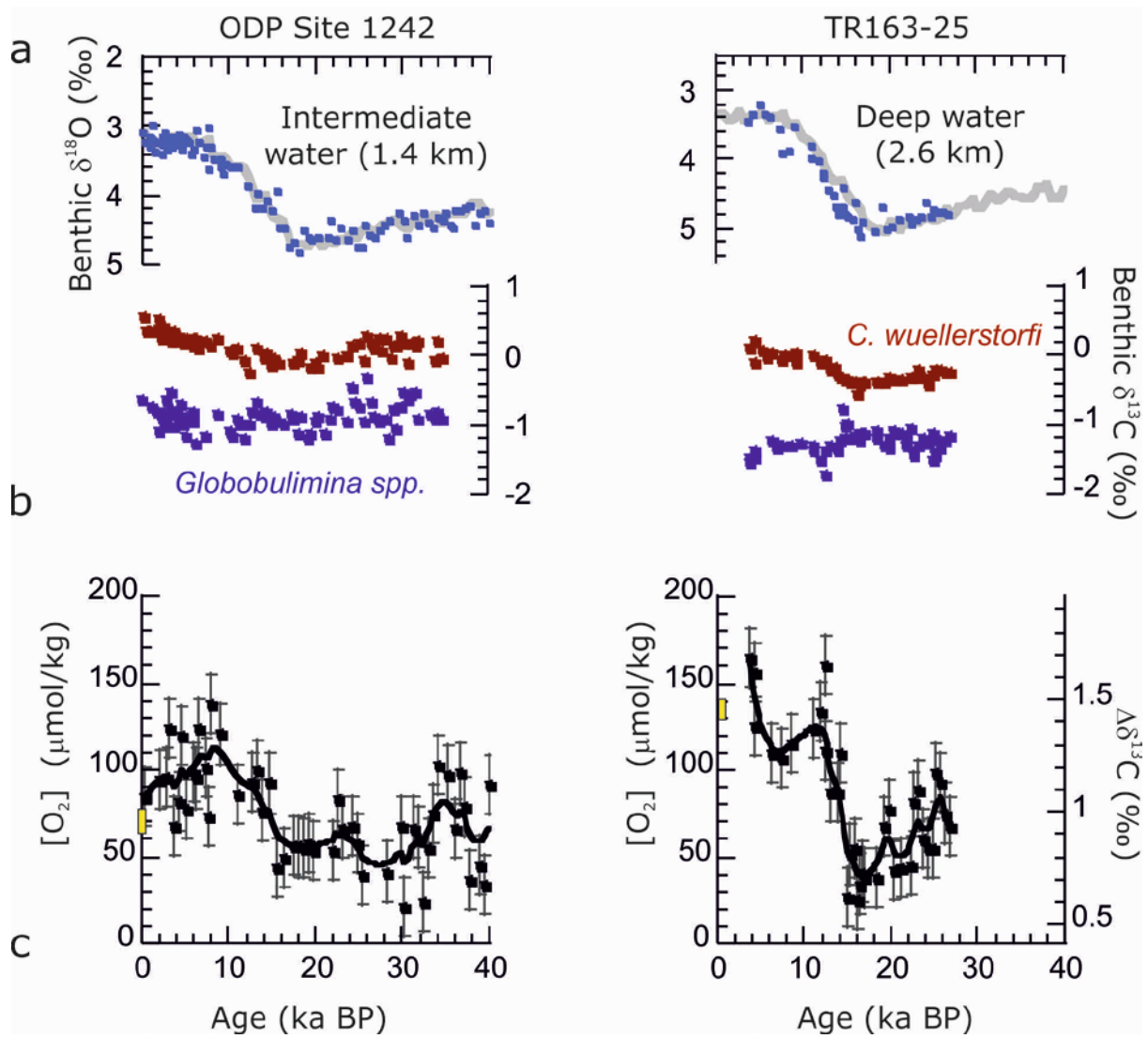
342

343



344

345



METHODS

Analytical methods

Foraminifera oxygen and carbon isotopes for ODP Site 849 and 1242 were measured using a Thermo MAT253 IRMS coupled to a Kiel Device at the Godwin Laboratory (University of Cambridge) and a Thermo Delta V Advantage coupled to a Kiel Device at the Department of Earth Sciences (University of Oxford). Calibration to VPDB was via NBS19 standards. Overall precision for $\delta^{18}\text{O}$ is $\sigma=0.07\text{‰}$ (Oxford) and $\sigma=0.08\text{‰}$ (Cambridge), and for $\delta^{13}\text{C}$ is $\sigma=0.04\text{‰}$ (Oxford) and $\sigma=0.06\text{‰}$ (Cambridge). For benthic foraminifera analyses we typically used 3-5 specimens of *C. wuellerstorfi*, 6 specimens of *C. pachyderma*, and > 4 specimens of *Globobulimina* spp. For planktonic foraminifera analyses a minimum of 20 specimens were analysed. For site TR163-25 benthic foraminifera oxygen and carbon isotopes, as well as (homogenized) bulk sedimentary nitrogen isotopes, were carried out on a GV Isoprime stable isotope ratio mass spectrometer at the University of South Carolina, with a long-term lab reproducibility of 0.07‰ (oxygen) 0.06‰ (carbon), and 0.14‰ (nitrogen). Typically 1-5 *Globobulimina* spp. and *C. wuellerstorfi* were used for benthic foraminifera stable isotope analyses at site TR163-25.

Planktonic foraminifera I/Ca ratios were measured by quadrupole ICP-MS (Bruker M90) at Syracuse University, using the method of³. The sensitivity of iodine was tuned to above 80 kcps for a 1 p.p.b. standard. Iodine calibration standards were freshly prepared from KIO_3 powder. The precision for ^{127}I is typically better than 1%. The detection limit of I/Ca is on the order of 0.1 $\mu\text{mol/mol}$.

369

370 **Age models**

371 The age models for ODP 849 and 1242 are based on oxygen isotope stratigraphy, matching
372 new benthic foraminiferal $\delta^{18}\text{O}$ records (Fig. 2, 3) to the Pacific intermediate and deep
373 stacked $\delta^{18}\text{O}$ records of Stern and Lisiecki²³.

374 Age control points ODP 1242 & 849:

Depth (cm) 1242	Age (ka BP) 1242		Depth (cm) 849	Age (ka BP) 849
0	0		13	6
191	11		37	10
196	13		61	17.5
255	17			
461	30.5			
565	38			

375

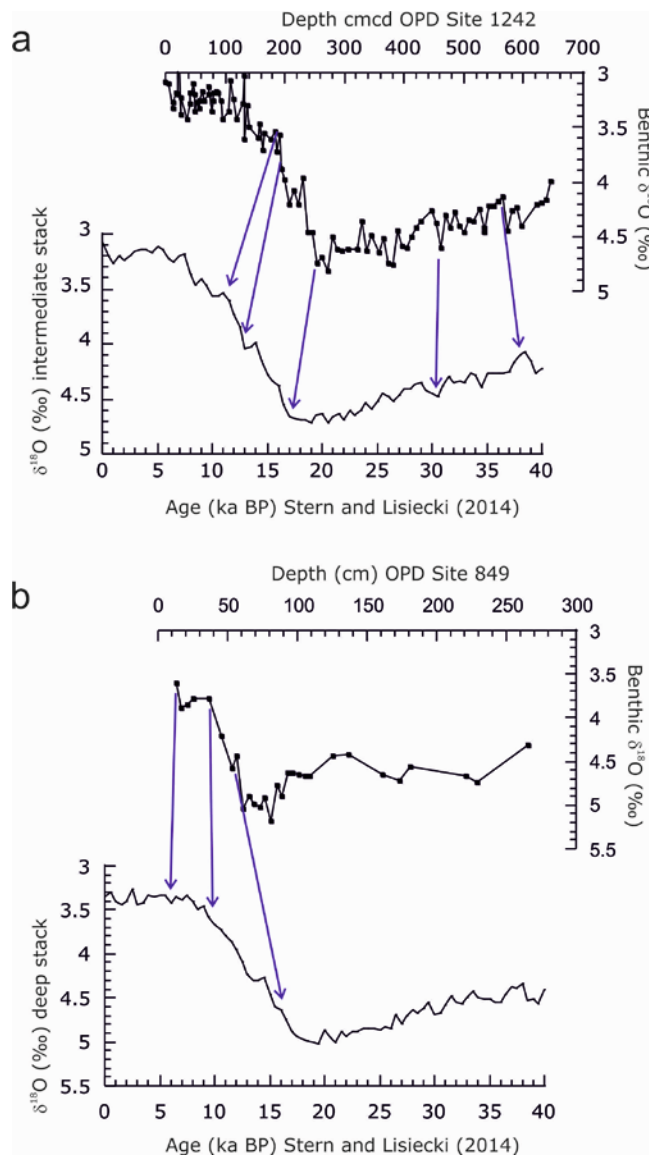


Figure 4. Age control points for ODP Site 1242 (a) and 849 (b).

For TR163-25 the existing chronology of 31 was used, which was developed using 4 *N. dutertrei* ^{14}C ages calibrated with reservoir ages calculated for the EEP from TR163-23 and ODP1240³⁰ using the Bayesian age model program BACON³².

Bottom water oxygen concentrations

Hoogakker et al.⁴ show there is a strong ($R^2 = 0.94$) linear relationship between bottom water oxygen concentrations and $\Delta\delta^{13}\text{C}$ at oxygen levels between 55 and 235 $\mu\text{mol/kg}$, with a $\sim 0.4\text{‰}$ increase in $\Delta\delta^{13}\text{C}$ for every 50 $\mu\text{mol/kg}$ increase in bottom water oxygen concentrations. According to⁴, the total error associated with bottom water oxygen concentration at mid- to low latitudes is $\pm 17 \mu\text{mol/kg}$. When oxygen concentrations exceed 255 $\mu\text{mol/kg}$, the relationship with $\Delta\delta^{13}\text{C}$ weakens due to $\delta^{13}\text{C}$ of *Globobulimina* spp. becoming much more depleted. This typically occurs in environments where the oxygen penetration depth is deeper than the sediment mixed layer causing addition of light carbon through sulphate reduction²¹. At oxygen concentrations between 50 and 20 $\mu\text{mol/kg}$ we expect the strong linear relationship ($\Delta\delta^{13}\text{C} = 0.00772 * [\text{dissolved oxygen concentration}] + 0.41446$) to hold, as aerobic respiration still dominates the remineralization of organic carbon³³. This is supported by 2 new data points derived from temperate North Pacific Holocene samples of ODP Sites 1014 ($[\text{O}_2] = 32 \pm 10 \mu\text{mol/kg}$; $\Delta\delta^{13}\text{C} = 0.54 \pm 0.03\text{‰}$) and 1019 ($[\text{O}_2] = 21 \pm 6 \mu\text{mol/kg}$; $\Delta\delta^{13}\text{C} = 0.44 \pm 0.1\text{‰}$). At ODP Site 1242, products of manganese and iron reduction (Mn^{2+} and Fe^{2+})³⁴ become important below 50 meters composite depth (reconstructions of $\Delta\delta^{13}\text{C}$ only took place between 0 and 6.5 m). Therefore, we do not expect deviations in $\Delta\delta^{13}\text{C}$ in relation to these processes.

Subsurface water oxygen concentrations

To document upper ocean oxygenation, we use the planktonic foraminifera I/Ca proxy of Lu et al. (2016)³. The electrode potential of the iodate/iodide couple is very similar to that of denitrification³⁵. In the surface ocean iodide exists in well oxygenated settings, which has been attributed to disequilibrium caused by biological activity and photochemical reduction

of iodate to iodide³⁶⁻³⁸. The oxidation of iodide back to iodate is slow and may take from months to up to 40 years²⁰.

I/Ca ratios were measured on several planktonic foraminifera species covering a range of depth habits. Spinose species *Globigerinoides sacculifer* (ODP 849, 1242) and *G. ruber* (ODP 1242) typically live in the surface mixed layer, whereas non-spinose species *Pulleniatina obliquiloculata* (ODP 849), *Globorotalia menardii* (ODP 1242), and *Neogloboquadrina dutertrei* (ODP 849, 1242) live deeper, at or below the thermocline³⁹⁻⁴¹. These depth habitat differences are expressed in the oxygen isotopes records, with consistently depleted values for the warmer surface mixed layer species, and heavier values for the deeper and cooler water dwelling species (Fig. 2). Pristine planktonic foraminifera were rigorously cleaned using the cleaning method of Barker et al. (2003)⁴² prior to I/Ca analyses.

It is unlikely that lower deglacial I/Ca ratios at ODP 849 are due to productivity changes; modern open ocean productivity pulses do not lower IO_3^- to concentrations below 0.25 $\mu\text{mol/l}$ in oxygenated water, suggesting that our planktonic foraminifera I/Ca signals are most likely driven by subsurface water oxygen concentrations and not productivity³.

Nitrogen isotopes

Bulk sedimentary $\delta^{15}\text{N}$ can indirectly reflect the extent of suboxia within the upper water column, near the core site, due to the enrichment of ^{15}N in residual nitrate during denitrification⁴³. Nitrogen isotopes can however also be affected by other processes such as dilution of the isotopic signal given the fraction of nitrate consumed by denitrification in suboxic zones⁴⁴, the input of nitrate by advection from distant suboxic zones¹⁶, the addition of

low ^{15}N nitrogen by N_2 fixation, and partial nitrate uptake by phytoplankton at remote locations^{18, 45}, and so are not unambiguous recorders of the local extent of suboxia.

Bulk sedimentary $\delta^{15}\text{N}$ at both ODP Site 1242 (Fig. 2) and TR163-25 (Fig. 5) show lower values during the LGM, consistent with other $\delta^{15}\text{N}$ records within the region¹⁸. Only at ODP Site 1242 are sufficiently-low oxygen concentrations ($[\text{O}_2] < 2\text{-}4 \mu\text{mol/kg}$) found for denitrification to occur today⁴⁶, and only at more than 300 m depth in the water column (Fig. 1). This is below the depth from which wind-driven upwelling draws. Thus, the nitrogen incorporated in organic matter at the surface and exported to depth, producing the bulk sedimentary $\delta^{15}\text{N}$ record, does not directly reflect local suboxia at either site. Instead, the records at these locations are likely to reflect regional changes in nitrogen cycling, as is true for the similar records found throughout the ETP¹⁸. These changes could have included lower rates of denitrification despite similar volumes of OMZ waters, or more complete nitrate consumption during denitrification leading to a weaker isotopic signal.

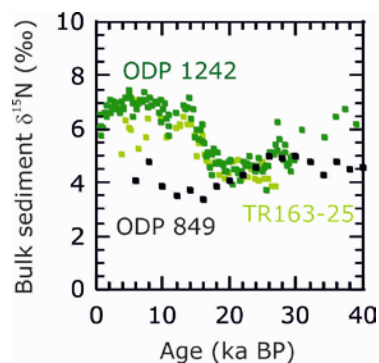


Figure 5. Bulk sedimentary $\delta^{15}\text{N}$ plotted against age for ODP Sites 1242⁴⁷, 849⁴⁸, and TR163-25 (this work).

Notably, nitrogen isotope values at the Gulf of Tehuantepec, where the most active water column denitrification occurs today, were similar during the LGM and late Holocene (7‰) consistent with similarly active denitrification during both times¹⁷.

Changes in the soft tissue pump

The $\delta^{13}\text{C}$ value of dissolved inorganic carbon ($\delta^{13}\text{C}_{\text{DIC}}$) depends on both the preformed component ($\delta^{13}\text{C}_{\text{pre}}$) and soft tissue components ($\delta^{13}\text{C}_{\text{soft}}$). The latter term results from the remineralization of organic matter and is related through stoichiometric ratios to oxygen consumption and carbon storage. The $\delta^{13}\text{C}_{\text{pre}}$ is determined by temperature, salinity, pCO_2 , alkalinity, the whole ocean average $\delta^{13}\text{C}$, and the disequilibrium of surface waters when they sink. Often overlooked, the $\delta^{13}\text{C}_{\text{pre}}$ value is sensitive to changes in the soft tissue pump in addition to globally-averaged $^{13}\text{C}/^{12}\text{C}$.

If we ignore the small impact of the carbonate pump on carbon isotopes, the $\delta^{13}\text{C}_{\text{DIC}}$ at an arbitrary point in the ocean interior is given by

$$\delta^{13}\text{C}_{\text{DIC}} = (\delta^{13}\text{C}_{\text{pre}} \times \text{DIC}_{\text{pre}} + \delta^{13}\text{C}_{\text{soft}} \times \text{DIC}_{\text{soft}}) / \text{DIC}_{\text{tot}} \quad \text{eq. 1}$$

The LGM-Holocene change (D) in all quantities is approximately:

$$D\delta^{13}\text{C}_{\text{DIC(LGM-Hol)}} = D(\delta^{13}\text{C}_{\text{pre}} \times \text{DIC}_{\text{pre}}) / \text{DIC}_{\text{tot}} + D(\delta^{13}\text{C}_{\text{soft}} \times \text{DIC}_{\text{soft}}) / \text{DIC}_{\text{tot}} \quad \text{eq. 2}$$

This equation includes a number of unknowns, that can be simplified using three assumptions. First, that changes in $\delta^{13}\text{C}_{\text{soft}}$ were negligible. Second, that although the shallow and deep sites certainly would have had different preformed components, the glacial-interglacial change in the preformed component, $D(\delta^{13}\text{C}_{\text{pre}} \times \text{DIC}_{\text{pre}})$, was the same at the two

sites. Third, that the change in $DIC_{\text{soft}}/DIC_{\text{tot}}$ was small. This then gives change in $\delta^{13}C_{\text{pre}}$ between the two depths in (z2-z1) as:

$$D\delta^{13}C_{DIC(z2-z1)} = \delta^{13}C_{\text{soft}} \times DDIC_{\text{soft}(z2-z1)} / DIC_{\text{tot}} \quad \text{eq. 3}$$

The $\delta^{13}C_{DIC}$ data show that the relative change between the deep and shallow site changes from 0.2‰ during recent times to -0.3‰ during the LGM, a change of 0.5‰. Assuming $\delta^{13}C_{\text{soft}}$ is -23‰ and DIC is about 2200,

$$-0.5 = (-23) \times (DDIC_{\text{soft}} / 2200)$$

$$\Delta DIC_{\text{soft}} = 48$$

This would imply a glacial-interglacial relative change in oxygen utilization between the two depths of $48 \times 140 [O_2] / 106 C = 63 \mu M$. Our new reconstructions show that oxygen concentrations at the two depths converged at the LGM. At present, oxygen concentrations at the deeper site are ~65 μM higher than the shallow site, which would imply that, based on the $\delta^{13}C$, oxygen concentrations during the LGM should have been the same at the two sites. This is essentially what we observe, supporting the assumption of similar changes in the preformed components in the waters bathing the two depths. Note that this is not to say that the preformed components were constant. Rather, they both changed considerably, but in a coordinated way, due to the whole ocean change of 0.34‰, and complex interconnected changes in temperature, alkalinity, salinity, pCO₂ and air-sea exchange dynamics. Because those changes appear to have changed in concert at these depths, we can then take the

assumption that, for the Pacific between ~1-3 km depth, there was a uniform LGM-recent change in $\delta^{13}\text{C}_{\text{pre}}$. As a result, the relative changes in $\delta^{13}\text{C}$ between sites should have been dominated by DIC_{soft} changes, allowing a large-scale budget to be constructed.

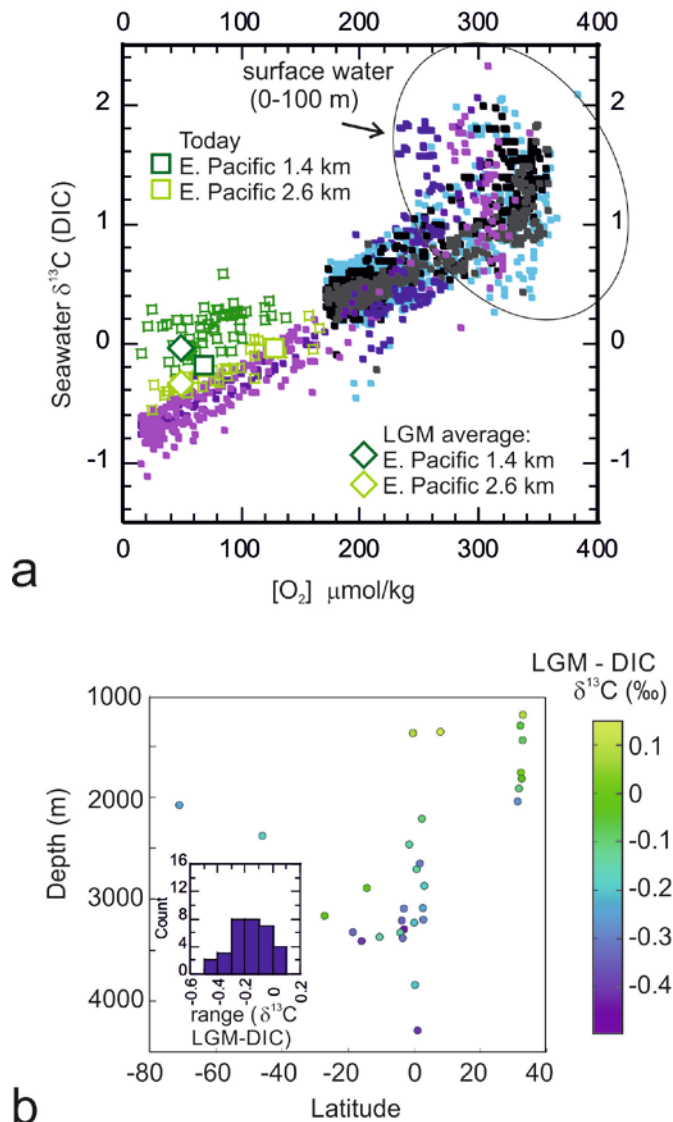


Figure 6. a Dissolved oxygen concentration (modern: dark blue: North Atlantic north of 50°N, light blue: South Atlantic south of 50°S, black/grey: Southeast/Southwest Pacific south of 50°S, dark purple/light purple: Northeast and Northwest Pacific north of 50°N; and reconstructed (last 40 kyr, dark green ODP Site 1242, mustard green TR163-25) plotted against carbon isotopes of DIC (‰) of seawater (data from

<https://www.nodc.noaa.gov/OC5/SELECT/dbsearch/dbsearch.html>. Square boxes represent modern values at the two sites, whereas diamonds represent LGM values (average 18-22 ka BP). **b** Latitudinal profile of the difference in Pacific carbon isotopes between the LGM (18-22 kyrs, from epifaunal benthic foraminifera) and recent (DIC) seawater carbon isotopes (extrapolated from²⁵). Inset: histogram of LGM- DIC $\delta^{13}\text{C}$ (waters deeper than 1.3 km) shows normal distribution (0.1 ‰ bin-width).

Between 1.4 and 3 km the average LGM-Recent $\delta^{13}\text{C}$ of DIC difference is $-0.10 \pm 0.13\text{‰}$. At TR163-25, LGM $\delta^{13}\text{C}$ was 0.30‰ lower than at present, while dissolved oxygen values were decreased by 65 $\mu\text{mol/kg}$ compared with recent times (Fig. 6). With our new constraints, the average decrease of 0.10‰ in LGM-Recent $\delta^{13}\text{C}$ of DIC between 1.4 and 3 km in the Pacific can be translated to oxygen concentrations that were 22 $\mu\text{mol/kg}$ lower ($(-0.10/0.30) \times 65$) than preindustrial. Assuming a 2.5 °C decrease in average deep Pacific temperature and a 1 unit increase in salinity (e.g. Adkins et al. (2002)⁴⁹), the saturated dissolved oxygen concentration (calculated using the equations of⁴⁵⁰) would be 353 $\mu\text{mol/kg}$, nearly 20 $\mu\text{mol/kg}$ higher than at present. Apparent oxygen utilization (difference between saturation oxygen concentration and measured oxygen concentration) was therefore increased by 42 $\mu\text{mol/kg}$ during the LGM in the deep Pacific. Extrapolated across water depths between 1.4 and 3 km this amounts to an increase in respired carbon of 90 Gt C. If similar conditions apply across the whole of the deep Pacific (all depths > 1.4 km), then the increase in respired carbon would amount to 196 Pg C (average LGM-Recent $\delta^{13}\text{C}$ of DIC difference is $-0.17 \pm 0.18\text{‰}$).

References METHODS:

31. Umling, N.E., Thunell, R.C. Synchronous deglacial thermocline and deep-water ventilation in the eastern equatorial Pacific. *Nat. Comm.* **8**, 14203 (2017).

32. Blaauw, M., Christen, J.A. Flexible paleoclimate age-depth models using an autoregressive gamma process. *Bayesian Anal.* **6**, 457-474 (2011).
33. Codispotti, L., Yoshinari, T., Devol, A.H. Suboxic respiration in the oceanic water column. In: *Respiration in Aquatic Ecosystems*, doi:10.1093/acprof:oso/9780198527084.001.0001 (2005).
34. Mix, A.C., Tiedemann, R., Blum, P., et al. *Proc. ODP Init. Rep.*, 202 (2003).
35. Lam, P., Kuypers, M.M.M. Microbial nitrogen cycling processes in oxygen minimum zones. *Ann. Rev. Mar. Sci.* **3**, 317-345 (2011).
36. Chance, R., Weston K., Alex R. Baker, A.R., Hughes, C., Malin, G., et al. Seasonal and interannual variation of dissolved iodine speciation at a coastal Antarctic site. *Mar. Chem.* **118**, 171-181(2010).
37. Spokes, L.J., Liss, P.L. Photochemically induced redox reactions in seawater, II. Nitrogen and iodide. *Mar. Chem.* **54**, 1-10 (1996).
38. Chance, R., Baker, A.R., Carpenter, L., Jickells, T.D. The distribution of iodide at the sea surface. *Environm. Sci. -Proc. Imp.* **16**, 1841- 1859 (2014).
39. Fairbanks, R.G., Sverdløve, M., Free, R., Wiebe, P.H., Bé, A.W.H. Vertical distribution and isotopic fractionation of living planktonic foraminifera in the Panama Basin. *Nature* **298**, 841-844 (1982).
40. Ravelo, A.C., Fairbanks, R.G. Oxygen isotopic composition of multiple species of planktonic foraminifera: recorders of modern photic zone temperature gradient. *Paleoceanography* **7**, 815-831 (1992).
41. Farmer, E.C., Kaplan, A., de Menocal, P.B., Lynch-Stieglitz, J. Corroborating ecological depth preferences of planktonic foraminifera in the tropical Atlantic with the stable

isotope ratios of core top specimens. *Paleoceanography* **22**, doi:10.1029/2006PA001361 (2007).

42. Barker, S., Greaves, M., Elderfield, H. A study of cleaning procedures used for foraminiferal Mg/Ca paleothermometry. *G-cubed* **4**, 8407 (2003).

43. Altabet, M.A., Pilskahn, C., Thunell, R., Pride, C., Sigman, D., Chavez, F., Francois, R. The nitrogen isotope biogeochemistry of sinking particles from the margin of the Eastern North Pacific. *Deep-Sea Res. I* **46**, 655-679 (1999).

44. Deutsch, C., Sigman, D.M., Thunell, R.C., Meckler, A.N., Haug, G.H. Isotopic constraints on glacial/interglacial changes in the oceanic nitrogen budget. *Global Biogeochem. Cy.* **4**, 1-22 (2004).

45. Farrell, J.W., Pedersen, T.F., Calvert, S.E., Nielsen, B. Glacial-interglacial changes in nutrient utilization in the equatorial Pacific Ocean. *Nature* **377**, 514-517 (1995).

46. Devol, A.H. Denitrification including Anammox. In Capone, D.G. et al. Eds. *Nitrogen in the Marine Environment* (2nd Edition), pp **263-301** (2008).

47. Robinson, R.S., Martinez, P., Pena, L.D., Cacho, I. Nitrogen isotope evidence for deglacial changes in nutrient supply in the eastern equatorial Pacific. *Paleoceanography* **24**, PA4213 (2009).

48. Rafter, P.A., Charles, C.D. Pleistocene equatorial Pacific dynamics inferred from the zonal asymmetry in sedimentary nitrogen isotopes. *Paleoceanography* **27**, PA3102 (2012).

49. Adkins, J.F., McIntyre, K., Schrag, D.P. The salinity, temperature and $\delta^{18}\text{O}$ of the glacial deep ocean. *Science* **298**, 1769-1773 (2002).

576 50. Debelius, B., Gómez-Parra, A., Forja, J.M. Oxygen solubility in evaporated seawater as a
577 function of temperature and salinity. *Hydrobiologia* **632**, 157-165 (2009).

578

579 Data availability

580 Data generated during our study have been deposited in Pangaea.de, and will be made
581 available upon publication of the manuscript.